# 2D Mixed-Matrix Membranes Based on Boron Nitride Nanosheets and Polyamide (PA) for Effective Gas Separation

**Barun Kumar Mondal ***
Assistant Professor,
Department of Chemistry,
Narajole Raj College, Vill: Narajole, PO: Harirajpur, Paschim Medinipore, West Bengal, India, Pin: 721211

## Abstract

Compared with traditional separation methods, membrane-based technology shows advantages in energy efficiency for natural gas purification. To overcome the performance trade-off of conventional polymeric membranes, a new array of mixed-matrix membranes (MMMs) was engineered, integrating two dimensional nanosheets of 2D boron nitride nanosheets (BNNS), into polymers of semi-fluorinated aromatic polyamide (PA) to selectively separate $CO_2$ from $CH_4$. The inclusion of 2D boron nitride nanosheets (BNNS), significantly increases the affinity between $CO_2$ molecules and the fabricated MMMs. The selectivity and permeability of these molecules can be controlled by drilling various free volume with different sizes and functionalized factors in the edge of free volume. The $CF_3$ substituting PA membrane exhibited the highest gas permeability which could be attributed to the loose chain packing via the incorporation of the bulky $CF_3$ substituting group in polymer matrix. The PA matrix was filled with BNNS nanosheets at two different weight percentages: 2% and 4%. The 4 wt% MMM showed a $CO_2$ permeability and a selectivity of 36 for $CO_2/CH_4$, showing enhanced separation performance because of the submicron fillers. The homogeneous integration of BNNS nanosheets into the PA matrix was verified by SEM imaging. The present study is valuable for designing novel nanostructure membranes for gas separation.

**Index Terms - Poly(amide), Gas permeability, 2D boron nitride nanosheets, Mixed-matrix membranes.**

## 1. Introduction:

Natural gas has garnered a lot of attention as one of the world's most significant fuel sources. However, there is an unacceptable amount of $CO_2$ in raw natural gas, which needs to be eliminated. Environmental friendliness and energy efficiency are two benefits of membrane separation technology. [1-3] Unfortunately, the trade-off phenomenon, which states that high permeability and selectivity cannot be achieved. In gas separation, non-porous multilayer two-dimensional (2D) nanosheets have also surfaced as possible MMM fillers. Graphene oxide (GO) and graphitic carbon nitride are two examples of 2D sheets that have been added to polymer matrices. These enhancements provide a way to investigate the impact of additional 2D materials. An isostructural and isoelectric equivalent of graphene, boron nitride nanosheets (BNNS), have been integrated into PA in this study. [3-5] BNNS have several beneficial qualities, including as strong mechanical strength and superior resistance to oxidation and chemicals. Because of these characteristics, BNNS is a viable option for membrane technology in a variety of applications. For nanofiltration, MMMs of BNNS/polyethersulfone (PES) demonstrated no irreversible fouling and a four-fold increase in water permeance. By adjusting pore size and surface chemistry, BNNS membranes might improve $CO_2/N_2$ separation for gas separation applications, according to molecular dynamics simulations. [5-9] $H_2$ selectivity over other gases was significantly increased by adding amino-functionalized BNNS to polyimide nanocomposite membranes. This study examined the gas permeabilities of several gases, including $CO_2$, $O_2$, $N_2$, and $CH_4$, using innovative mixed matrix BNNS/PA membranes.

## 2. Experimental

### 2.1. Materials & Equipments

Commercial hexagonal boron nitride (h-BN) with mean flake size of 45 μm purchased from Sigma-Aldrich. There has been prior documentation on the process for producing 2,6-bis[3'-trifluoromethyl-4'(4"-carboxyphenoxy)benzyl]pyridine (2) acid. [2-4] The monomer of m-phenyl diamine was procured from SD Chemicals located in India. An automatic Diffusion Permeameter (DP-100-A) from Porous Materials, Inc., USA, was used to test the permeability of the gases $O_2$, $N_2$, $CO_2$ and $CH_4$ through the polymer membranes at 35 °C and an operating gas pressure of 3.5 bar.

### 2.1. Polymerization and membrane preparation

As shown in Scheme 1, triphenyl phosphite (TPP), $CaCl_2$, pyridine, and NMP were used as the solvent in a 1:1 molar ratio reaction between triphenylamine (1), an aromatic diamine, and a dicarboxylic acid monomer (2). The following is how the polymerization process (PY PA) was carried out: a mixture of diamine, m-triphenylamine (0.602 g, 5.60 mmol) (1), 2,6-bis[3'-trifluoromethyl-4'(4"-carboxyphenoxy)benzyl]pyridine (2) (0.320 g, 5.60 mmol), $CaCl_2$ (0.25 g), pyridine (1.2 mL), NMP (3 mL), and TPP (1.2 mL, 4.94 mmol) was heated in a round-bottom flask with a reflux condenser at 110 °C for six hours. This combination was then added to methanol, which caused a fibrous polymer to develop. The polymer was then vacuum-dried.

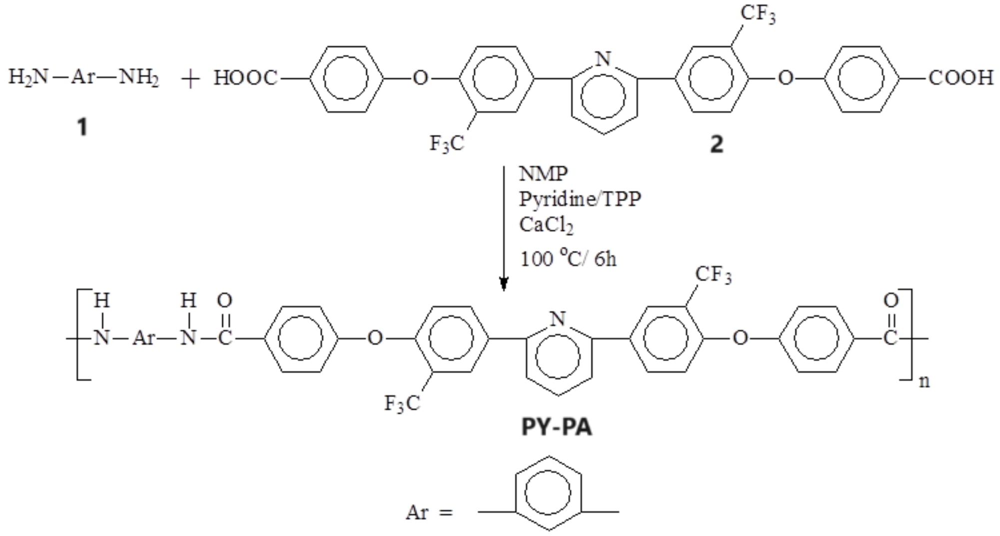

**Scheme 1: Preparation of the poly(amide)s (PY PA). [2-4]**

## BNNS nanosheets Synthesis

BNNS were fabricated by modifying a known liquid exfoliation method: IPA and ultrapure water were mixed 55:45 vol% and then employed as the solvent mixture. The commercial h-BN powder was dispersed in the solvent mixture to a concentration of 5 g $L^{-1}$. The suspension was sonicated (ultrasound bath, 45 kHz, 80W) overnight at 5 °C followed by centrifugation at 3,000 RPM for 20 min. The supernatant was further centrifuged at 4,900 RPM for 30 min. [9]

## Polymeric Membrane Preparation

For six hours, polymeric membranes were baked at 80 °C and 150 °C in glass Petri plates that had been cleaned. After being removed from the Petri dishes using hot water, the membranes were vacuum-dried for four hours at 160 °C. It was possible to create flexible membranes. Table 1 provides an overview of the physical attributes. After determining the density values (ρ), the fractional free volume (FFV) was computed using the formula $FFV = (V-1.3V_w)/V_w$, where V represents the specific volume ($V = 1/\rho$), density values (ρ). Hyperchem computer program was used for van der Waals volume ($V_w$) calculation. [3-5]

## Preparation of BNNS/PA MMMs

Using 0.6 g of polymer, a PA A solution was dissolved in DMF to prepare mixed matrix membranes (MMMs). Using ultrasonication, the BNNS nanosheets were distributed across DMF. After that, the polymer solution was added to the suspension of BNNS nanosheets, and it was agitated all night. After six hours of heating between 80 °C and 150 °C, the homogenous polymer solution was cast onto spotless glass Petri plates to create flexible, free-standing membranes. For MMMs, the filler weight ratio to the combined filler and polymer weight was maintained at a fixed level to guarantee consistency. BNNS nanosheet loadings of 2%, and 4% by weight of the fillers were used to make MMMs, enabling a methodical examination of the impacts of changing BNNS loading. [5-7]

## 3. Results and discussion

### 3.1. Polymer synthesis and their properties

The usual polycondensation-based phosphorylation method using dicarboxylic acid (2) and diamine (1) resulted in polyamide (**Scheme 1**). Verify polymer unit structures again using NMR. The $^1$H-NMR spectra and the polymer repeat unit structures agreed. PA A's pyridine-$d_5$ $^1$H-NMR spectra showed a singlet above 11.35 ppm (amide proton). Physical characteristics were discovered to be in line with our earlier results.

**Table 1. Physical properties of the polyamide**

| Polymer | $\eta_{inh}$ (dL g$^{-1}$)[a] | Density (g cm$^{-3}$)[b] | $V_w$ (cm$^3$ mol$^{-1}$)[c] | FFV |
|---|---|---|---|---|
| PA A | 0.42 | 1.341 | 313.7 | 0.121 |

[a]$\eta_{inh}$ = inherent viscosity at 30 °C. [b]Density measured at 30 °C. [c]$V_w$ = Vander Waals volume, FFV = Fractional Free Volume.

### 3.2 Morphology: Synthesis of BNNS nanosheet

BNNS were prepared by exfoliating h-BN via ultrasonication. Based on the available literature, the exfoliation of h-BN powder was attempted in different liquid systems (e.g. pure water, solvent, solvent mixtures) by ultrasonication in a bath, probe ultrasonication or microwave irradiation. Ultrasonication temperature and duration were also controlled, and it was observed that exfoliating h-BN in a mixture of solvents at low temperature in an ultrasonication bath. Therefore, exfoliation in ultrasonication bath was employed to produce large amounts of BNNS, followed by size fractionation by centrifuging the resulting suspension at different speeds. After the size fractionation process, the morphological characteristics of the exfoliated BNNS, including size and thickness were investigated using TEM. BNNS have an average lateral size of around 1 μm and thickness of around 4 nm, which is equivalent to about 12 layers. In Fig. 1 shows a typical hexagonal symmetry, which indicates the highly crystalline hexagonal lattice of boron nitride was not damaged during the liquid exfoliation process. [4-8] The surface chemistry of the initial *h*-BN material and the exfoliated BNNS were compared by FT-IR. Fig. 2 shows similar strong and broad peaks at ~ 1370 cm$^{-1}$ and ~ 820 cm$^{-1}$ corresponding to in-plane B–N transverse stretching vibration and out-of plane B–N–B bending vibration for both *h*-BN and BNNS.

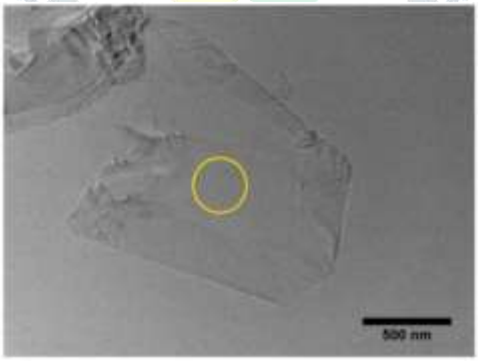

**Fig 1: TEM image of the exfoliated BNNS [4-8]**

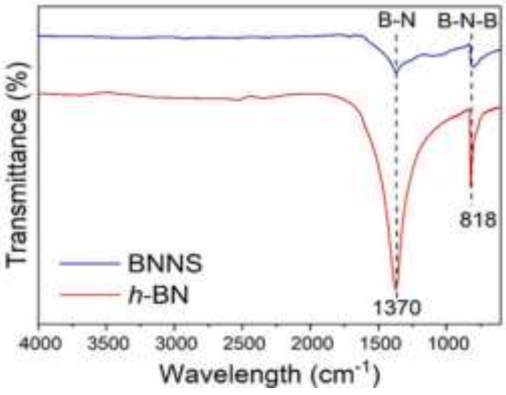

**Fig. 2. FT-IR spectra of h-BN and BNNS [4-8]**

### 3.3 Processing of Mixed Matrix Membranes

X-ray diffraction (XRD) patterns of the virgin PA A membrane and MMMs with BNNS fillings. There were noticeable large peaks on the PA A membrane at around 13.6º and 18º. The existence of BNNS in MMM is confirmed by the extra peak in the XRD patterns of the MMM samples, which is located about 26◦ and is ascribed to the (002) plane of BNNS. The SEM images in Figure 3 were used to analyze the microstructures of the membranes. As seen in Figure 3, the pure PA A membrane has a perfect top surface and a uniform, dense cross-section. The MMMs' micrographs show dense, defect-free layers devoid of any discernible filler agglomeration (Fig. 3, a-c). [5-9]

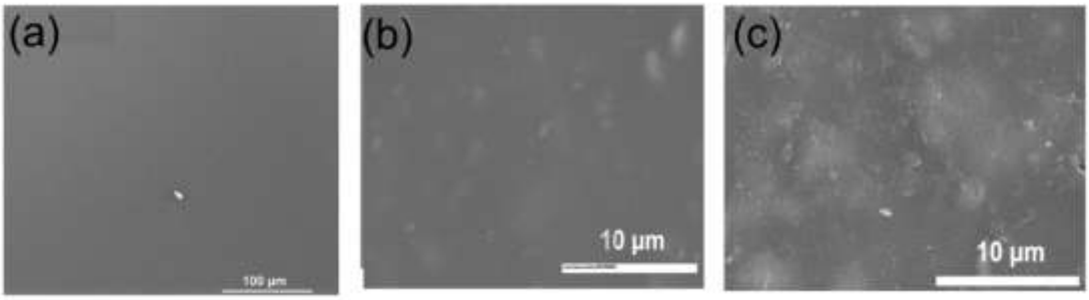

**Figure 3: SEM images of Pristine PA A membrane (a) with BNNS loading of (b & c) 2 wt % and 4 wt %. [5-9]**

### 3.4 Gas permeation

#### 3.4.1 Effect of BNNS on gas permeation properties

All MMMs underwent gas permeation testing at 293 K and 3.5 bar. As indicated in Table 2, the permeability of several gases ($O_2$, $N_2$, $CO_2$ and $CH_4$) across the membranes was measured using the constant-volume method. For these MMMs, the order of gas permeability is of P ($CO_2$) > P ($O_2$) > P ($N_2$) > P ($CH_4$). The solution-diffusion model, which has been extensively described in the literature, is followed by the transport mechanism. The PA membrane's permeability is greatly increased by the addition of BNNS nanosheets, and gas permeability rises as BNNS nanosheet concentration does (**Table 2**). The BNNS nanosheets' sieve action on the gas molecules is the cause of this improvement. The excellent particle dispersion in the MMMs is responsible for the increased $CO_2/CH_4$ selectivity as BNNS nanosheet loading increases from 0 weight percent to 4.0 wt%. The matrix contains mesopores that allow gas molecules to pass through, improving the optimal $CO_2/CH_4$ selectivity, suggesting that the addition of BNNS increases the tortuosity for gas molecules, slowing down diffusion and perhaps partially blocking some FFV of polymer. Although they are still below the 2008 Robeson $CO_2/CH_4$ upper bound. Nevertheless, with the addition of very small quantities of BNNS fillers, the drop in $CO_2$ permeability. [3-7]

**Table 2. Gas permselectivities and permeability of the MMMs.**

| MMMs | $P(CO_2)$ | $P(O_2)$ | $P(N_2)$ | $P(CH_4)$ | $\alpha(CO_2/CH_4)$ | $\alpha(O_2/N_2)$ |
|---|---|---|---|---|---|---|
| PA A | 65.0 | 12.2 | 1.59 | 1.54 | 36.50 | 7.86 |
| 2 wt. % -BNNS@PA A | 78.0 | 13.9 | 1.77 | 1.65 | 37.30 | 7.79 |
| 4 wt. % -BNNS@PA A | 80.0 | 14.1 | 1.91 | 2.33 | 44.20 | 9.13 |

P = gas permeability coefficient in barrer.

### 3.4.2 Corelation of gas permeabilities of MMMs with membranes

The permeability values and gas permeability of these MMMs (2–4 weight percent -BNNS@PA A) were compared to those of other polymers, including Ultem, Extem, and Matrimid. To have a better understanding, $CO_2/CH_4$ permselectivity vs $CO_2$ gas permeability was thoroughly evaluated using Robeson plots (Figure 4). The ability of the membrane to separate is indicated by the data points that touch Robeson's line. The MMMs often demonstrated a good mix of permeability and selectivity. Our membrane's permeability was higher than that of polymers that had already been reported. Although the overall performance of the MMMs did not surpass the Robeson upper bound, it was significantly enhanced. The 2 weight percent BNNS@PA A showed superior $CO_2$ gas permeability and increased permselectivity in comparison to PAs. The MMMs' greatest gas-separation performance was achieved at the highest loading of BNNS nanosheets (4 wt%), as shown by the fact that their Robeson trade-off points were near the upper bound. [37]

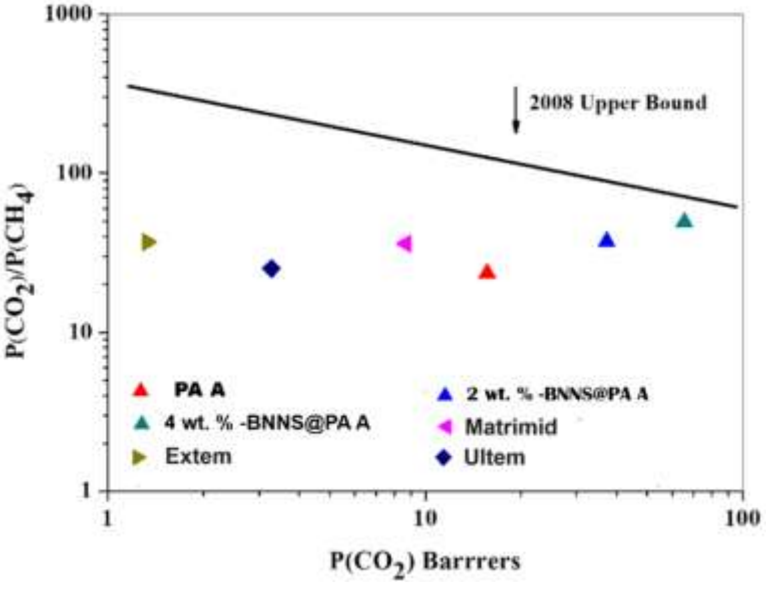

**Figure 4: Robeson plot of $CO_2/CH_4$ selectivity vs. $CO_2$ permeability [3]**

## 4. Conclusions

In conclusion, blended semi-fluorinated polyamide (PA A) with BNNS nanosheets using a solvent-evaporation technique to create a number of MMMs. The layered structure of BNNS nanosheets allowed the crystalline nanosheets to integrate smoothly into PA A, ensuring excellent interfacial compatibility. The MMMs with BNNS nanosheets showed constant filler dispersion and maintained excellent interfacial compatibility even at loadings up to 4 weight percent, which resulted in improved $CO_2$ permeability and $CO_2/CH_4$ selectivity. Among the membranes examined, the one with 2 weight percent BNNS performed the best and showed a discernible molecular sieving effect, with a $CO_2$ permeability of 80 Barrer and a $CO_2/CH_4$ selectivity of 44.2.

The preparation procedure ensured that PA A had a uniform distribution of BNNS nanosheets. Since BNNS nanosheets are more chemically compatible with PA A, higher quantities of these nanosheets were shown to improve permeability. The industrial use of this kind of MMM for natural gas sweetening is made possible by this work.

## 5. Acknowledgment

The author acknowledges Narajole Raj College for providing opportunity to carry out this work.

## 6. References

[1] Z. Tian, S. Wang, Y. Wang, X. Ma, K. Cao, D. Peng, X. Wu, H. Wu, Z. Jiang, Enhanced gas separation performance of mixed matrix membranes from graphitic carbon nitride nanosheets and polymers of intrinsic microporosity, J. Membr. Sci. 514 (2016) 15–24.

[2] D. Golberg, Y. Bando, Y. Huang, T. Terao, M. Mitome, C. Tang, C. Zhi, Boron nitride nanotubes and nanosheets, ACS Nano 4 (2010) 2979–2993.

[3] Banerjee, S., 2015. Handbook of specialty fluorinated polymers: Preparation, Properties, and Applications. William Andrew.

[4] Bisoi, S., Bandyopadhyay, P., Bera, D. and Banerjee, S., 2015. Effect of bulky groups on gas transport properties of semifluorinated poly (ether amide) s containing pyridine moiety. European Polymer Journal, 66, pp.419-428.

[5] V. Guerra, C. Wan, T. McNally, Thermal conductivity of 2D nano-structured boron nitride (BN) and its composites with polymers, Prog. Mater. Sci. 100 (2019) 170–186.

[6] D. Liu, L. He, W. Lei, K.D. Klika, L. Kong, Y. Chen, Multifunctional polymer/porous boron nitride nanosheet membranes for superior trapping emulsified oils and organic molecules, Adv. Mater. Interfaces 2 (2015) 1500228.

[7] Z.-X. Low, J. Ji, D. Blumenstock, Y.-M. Chew, D. Wolverson, D. Mattia, Fouling resistant 2D boron nitride nanosheet – PES nanofiltration membranes, J. Membr. Sci. 563 (2018) 949–956.

[8] J. Azamat, A. Khataee, F. Sadikoglu, Separation of carbon dioxide and nitrogen gases through modified boron nitride nanosheets as a membrane: insights from molecular dynamics simulations, RSC Adv. 6 (2016) 94911–94920.

[9] Y. Wang, Z.X. Low, S. Kim, H. Zhang, X. Chen, J. Hou, J.G. Seong, Y.M. Lee, G. P. Simon, C.H. Davies, Functionalized boron nitride nanosheets: a thermally rearranged polymer nanocomposite membrane for hydrogen separation, Angew. Chem. 130 (2018) 16288–16293.